Electronic Supplementary Information for:

Bipyridil-based chelator for Gd(III) complexation: kinetic, structural and relaxation properties

Szilvia Bunda,[§] Norbert Lihi,[†] Zsófia Szaniszló,[§] David Esteban-Gómez,[‡] Carlos Platas-Iglesias,[‡]* Mónika Kéri,[§] Gábor Papp[§] and Ferenc Krisztián Kálmán[§]**

[§]Department of Physical Chemistry, Faculty of Science and Technology, University of Debrecen, H-4032 Debrecen, Hungary

[†]ELKH-DE Mechanisms of Complex Homogeneous and Heterogeneous Chemical Reactions Research Group, Department of Inorganic and Analytical Chemistry, Faculty of Science and Technology, University of Debrecen, H-4032 Debrecen, Hungary

[‡]Centro de Investigacións Científicas Avanzadas (CICA) and Departamento de Química, Facultade de Ciencias, Univer-sidade da Coruña, 15071 A Coruña, Galicia, Spain

Table of content

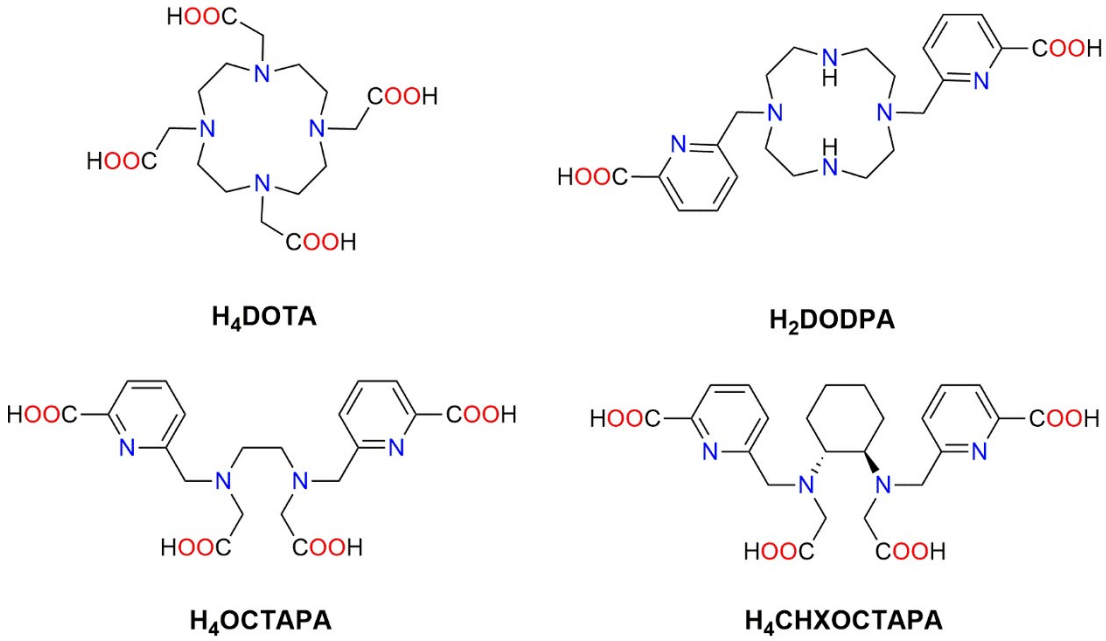

Scheme S1. Structure of the ligands mentioned in the text.

Synthesis of the ligand

Commercial reagents/solvents purchased from Sigma-Aldrich (St. Louis, MO, USA), Merck KGaA (Darmstadt, Germany) and Fluorochem Ltd. (Hadfield, United Kingdom) were used without further purification. The synthetic reactions were followed by Waters Alliance 2690 HPLC unit equipped with Waters 996 PDA detector, and a Phenomenex Luna C18(2) 100Å 150 x 4.6 mm 5 micron column. The preparative HPLC separations were carried out with a YL9100 HPLC system (Korea) equipped YL9101S degasser, YL9110S pump, YL9120S UV/VIS detector, Phenomenex Luna Prep C18(2) 100Å 250 × 21.2 mm 5 micron 00G-4252-P0-AX column and Sigma-Aldrich CHROMASOLV® Plus solvents. The NMR measurements were carried out with *Bruker* DRX *360 MHz and Bruker Avance I 400 MHz* spectrometers using deuterated solvents. Mass spectra were recorded on a maXis II UHR ESI-QTOF MS Bruker instrument in the Laboratory of Instrumental Analysis, Department of Inorganic and Analytical Chemistry of the University of Debrecen.

Tetraethyl 2,2',2'',2'''-(([2,2'-bipyridine]-6,6'-diylbis(methylene))bis(azanetriyl))tetraacetate (1): 0.55 g diethyl iminodiacetate (2.9 mmol, 2.4 eq), 1.25 g DIPEA (9.67 mmol, 8.1 eq.) and 0.04 g NaI (0.27 mmol, 0.23 eq.) were measured into a two-necked flask and dissolved in 60 mL dry acetonitrile. The flask was connected to a condenser and the mixture was heated to 60 °C. 0.3 g 6,6'-bis(chloromethyl)-2,2'-bipyridyl (1.19 mmol, 1.0 eq.) was measured into a dropping funnel in 20 mL dry acetonitrile. This mixture was added dropwise slowly to the hot reaction mixture which was stirred for 7 day. (The reaction was followed by analytical HPLC and MS methods). After completion of the reaction the hot mixture was filtered through a G3 glass filter and the solvent from the filtrate was removed under reduced pressure. The product was white powder (590 mg, 88 % yield) and used in the subsequent step without further purification.

2,2',2'',2'''-(([2,2'-bipyridine]-6,6'-diylbis(methylene))bis(azanetriyl))tetraacetic acid (H_4DIPTA): 0.47 g **(1)** (0.84 mmol, 1.0 eq) and 0.27 g NaOH (6.75 mmol, 8.0 eq.) was measured into a round-bottom flask and dissolved in 70 ml abs. EtOH. The flask was connected to a condenser and the mixture was heated to 60 °C. The reaction mixture was heated and stirred for 1 day. (The reaction was followed by analytical HPLC and MS methods). After completion of the reaction the hot mixture was filtered through a G3 glass filter and the solvent from the filtrate was removed under reduced pressure. The solid product was dissolved in 20 ml water and the pH of the solution was set to 2 with HCl when the yellowish product precipitated in crystalline form. The solid coumpound was washed multiple times with acidified water (0.25 g, 67 % yield). Its purity was investigated by HPLC and was found to be higher than 99% (see below).

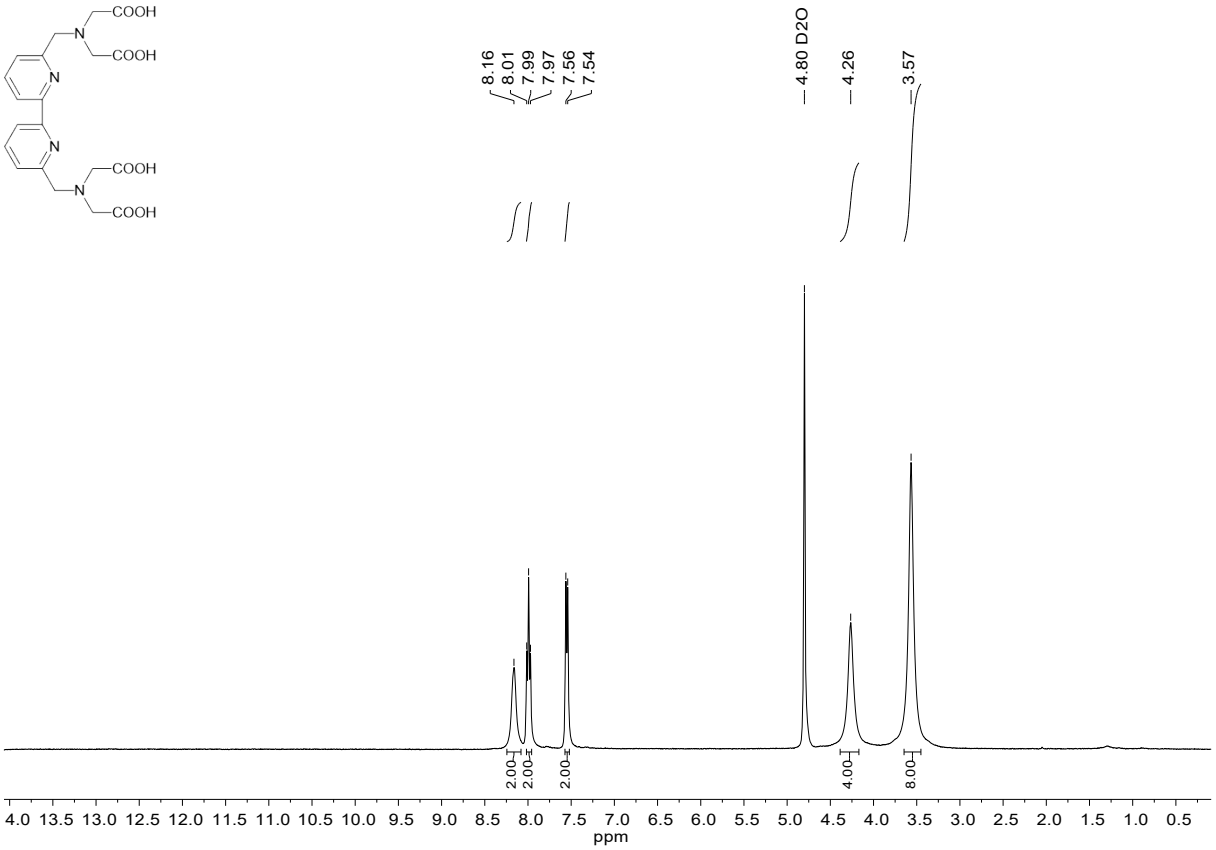

Figure S1. ^{1}H NMR spectrum of DIPTA ligand. ^{1}H-NMR (360 MHz, D_2O) δ (ppm): 3.57 (s, 8H), 4.26 (s, 4H), 7.55 (d, *J*=7.5 Hz, 2H), 7.99 (t, *J*=7.8 Hz, 2H), 8.16 (s, 2H).

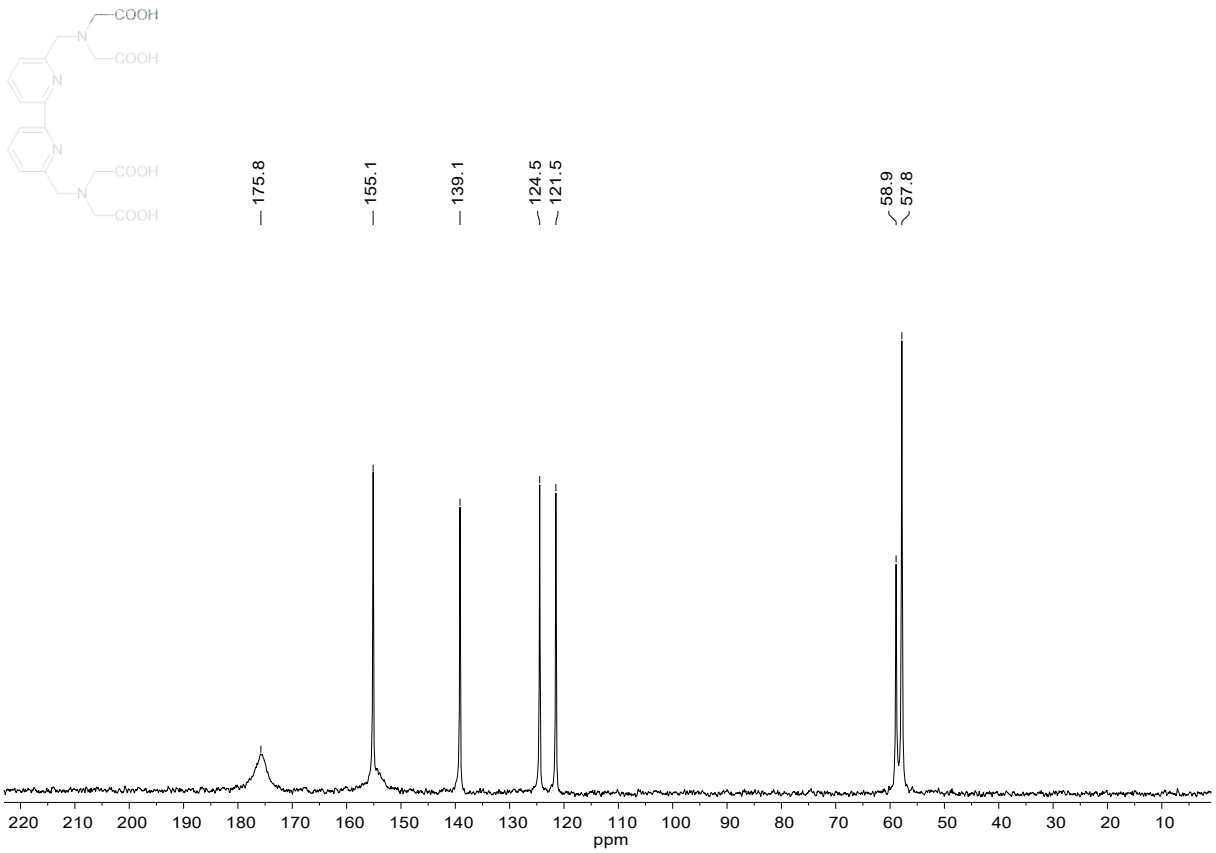

Figure S2. {^{1}H}-^{13}C NMR spectrum of DIPTA ligand. ^{13}C NMR (90 MHz, D_2O) δ (ppm): 57.8 (-*C*H_2-), 58.9 (-*C*H_2-), 121.5 (C_{ar}), 124.5 (C_{ar}), 139.1 (C_{ar}), 155.1 (C_q), 175.8 (-COOH).

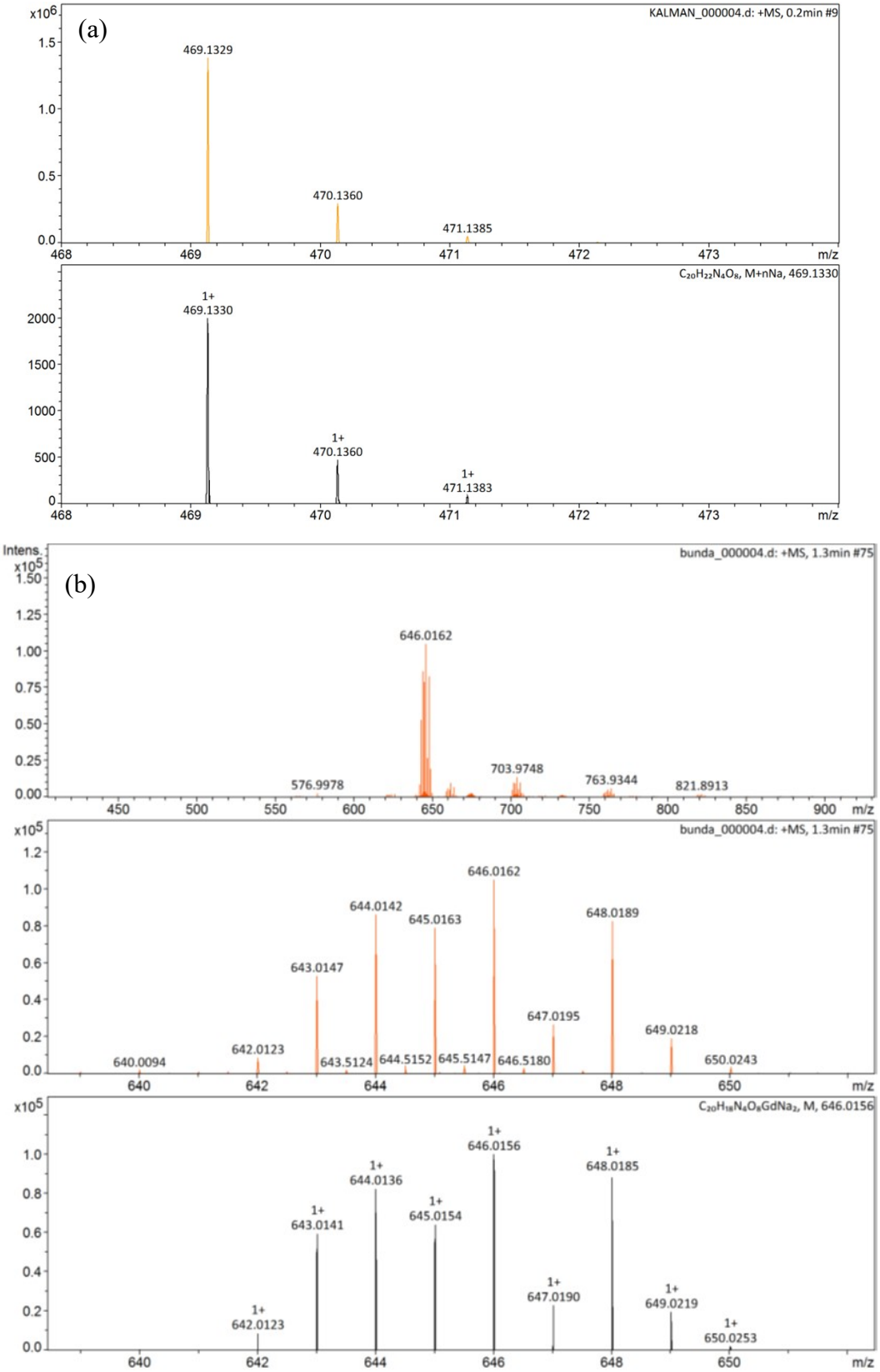

Figure S3. MS spectra of DIPTA (a) and $[Gd(DIPTA)]^-$ complex (b). ESI-HRMS (positive mode): (a) $[C_{20}H_{22}N_4O_8+Na]_{calc}$= 469.1329, $[C_{20}H_{22}N_4O_8+Na]_{found}$= 469.1330 (b) $[C_{20}H_{18}N_4O_8+Gd+2Na]_{calc}$ = 646.0156, $[C_{20}H_{18}N_4O_8+Gd+2Na]_{found}$ = 646.0162.

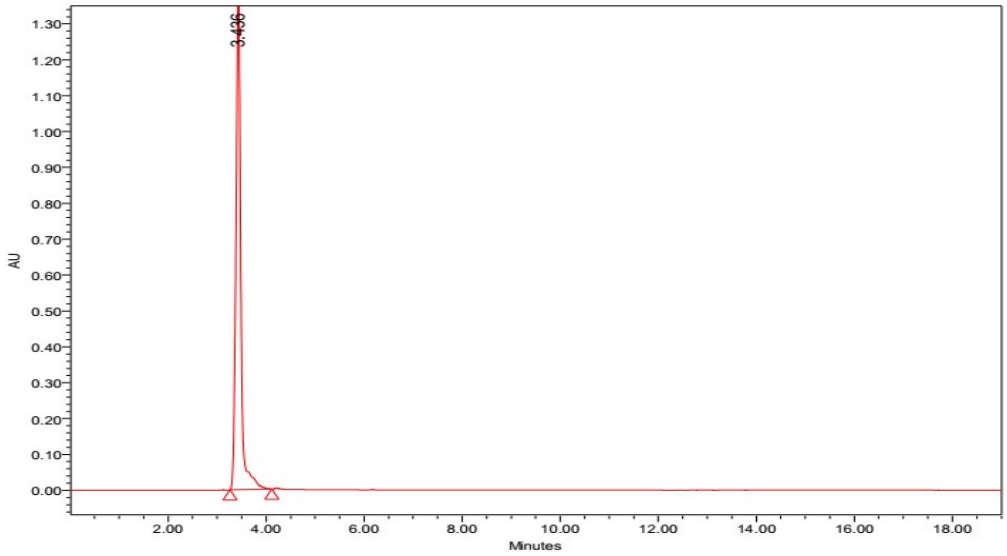

Figure S4. Analytical HPLC chromatogram of DIPTA ligand. Column: Phenomenex LUNA 5µm C18(2) 100Å 150 x 4.60 mm. Eluents: A: aqueous 5 mM TFA solution, B: ACN. Gradient: 5≺95% ACN 0≺15 min, 95≺5% ACN 15≺16 min, 5% ACN 16≺19 min. Flow: 1 mL/min. Retention time = 3.436 min. Purity > 99 %.

The ^{1}H, ^{13}C, HMBC, NOESY and COSY NMR spectra of the H_4DIPTA, $[Eu(DIPTA)]^-$ and $[Lu(DIPTA)]^-$:

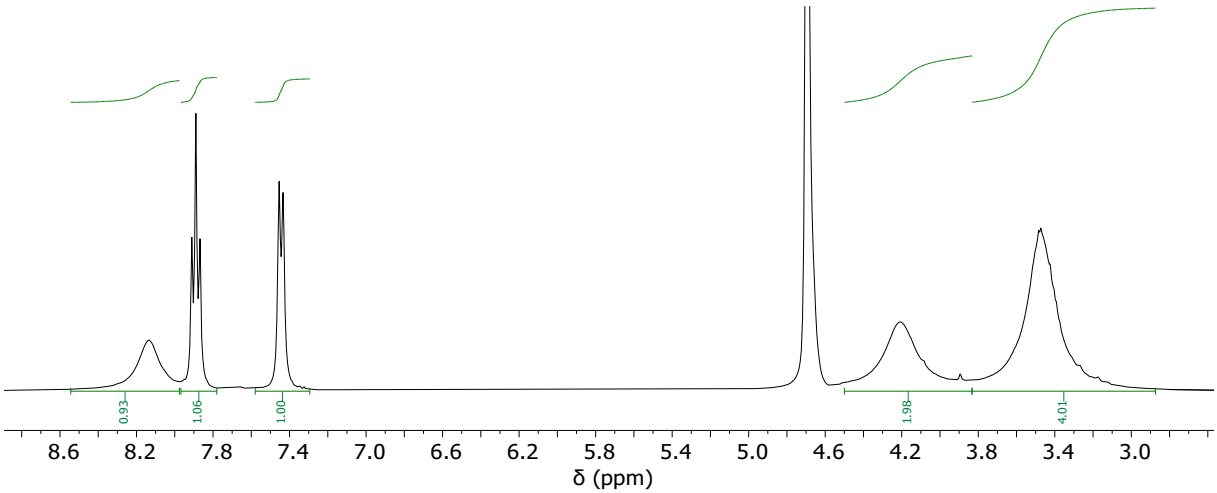

Figure S5. ^{1}H NMR spectrum of the H_4DIPTA ligand (pH=9.2, D_2O, T=298 K)

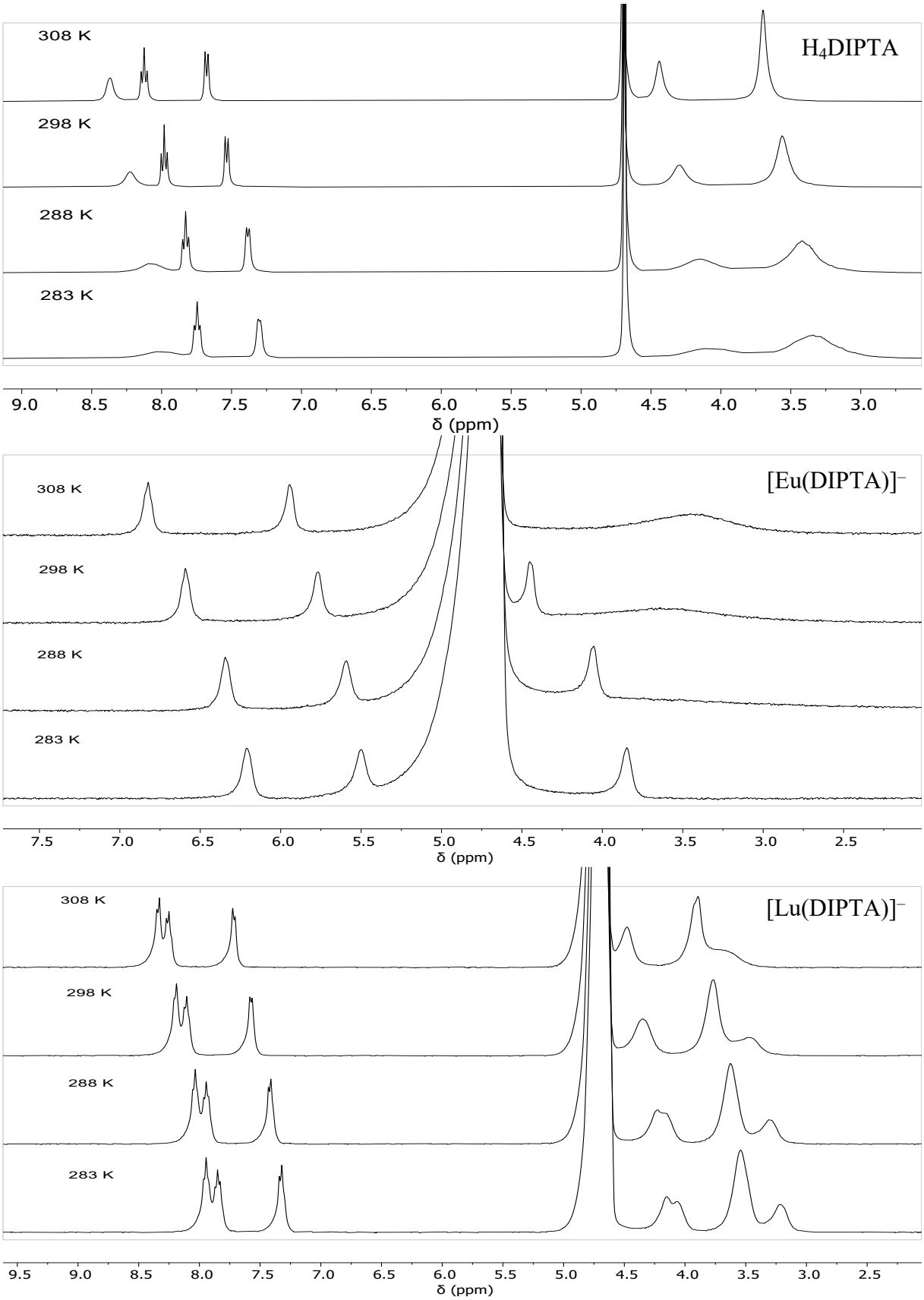

Figure S6. Temperature dependence of ^{1}H NMR spectra of the H_4DIPTA, $[Eu(DIPTA)]^-$ and $[Lu(DIPTA)]^-$ (pH=9.2, D_2O, T=283-308 K)

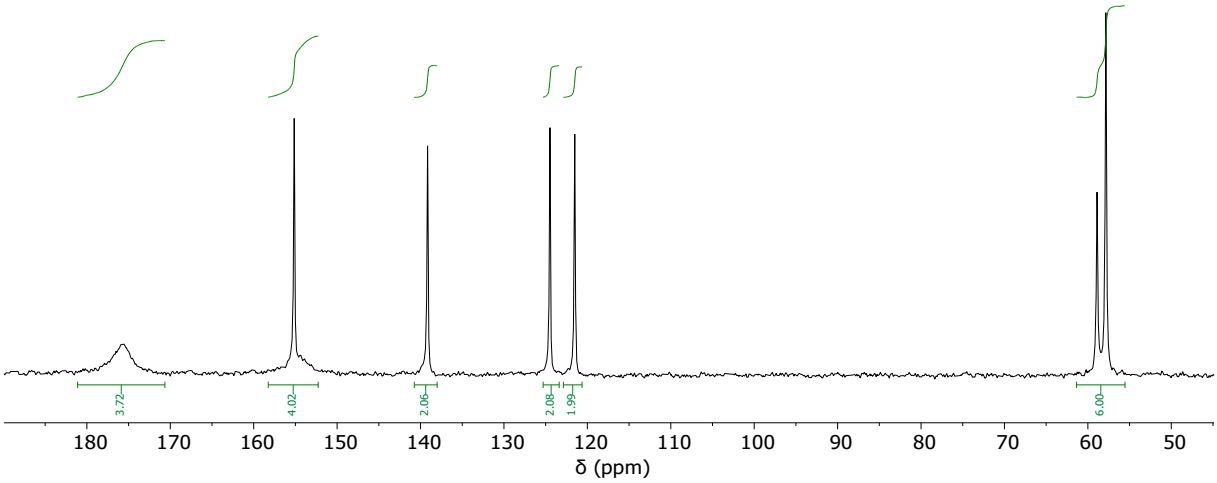

Figure S7. ^{13}C NMR spectrum of the H_4DIPTA ligand (pH=9.2, D_2O, T=298 K)

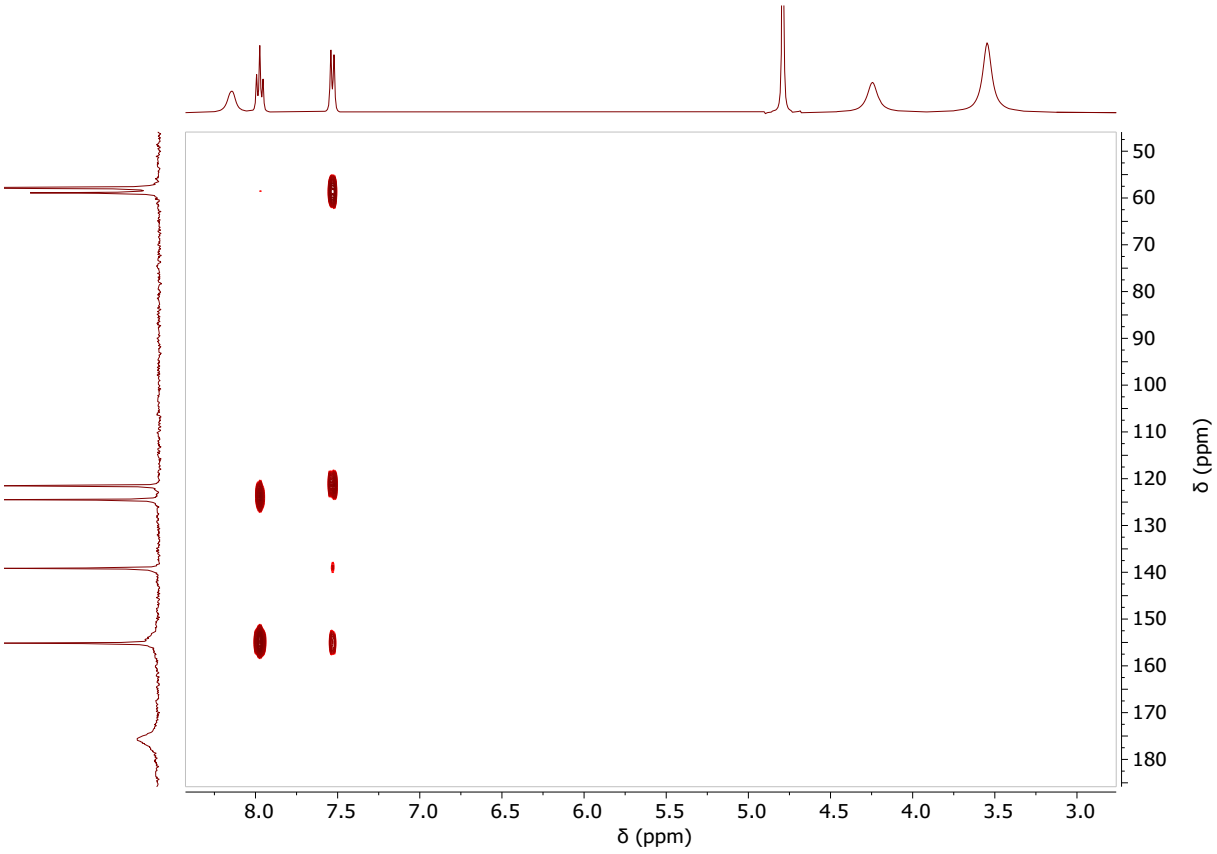

Figure S8. ^{1}H-^{13}C HMBC NMR spectrum of the H_4DIPTA ligand (pH=9.2, D_2O, T=298 K)

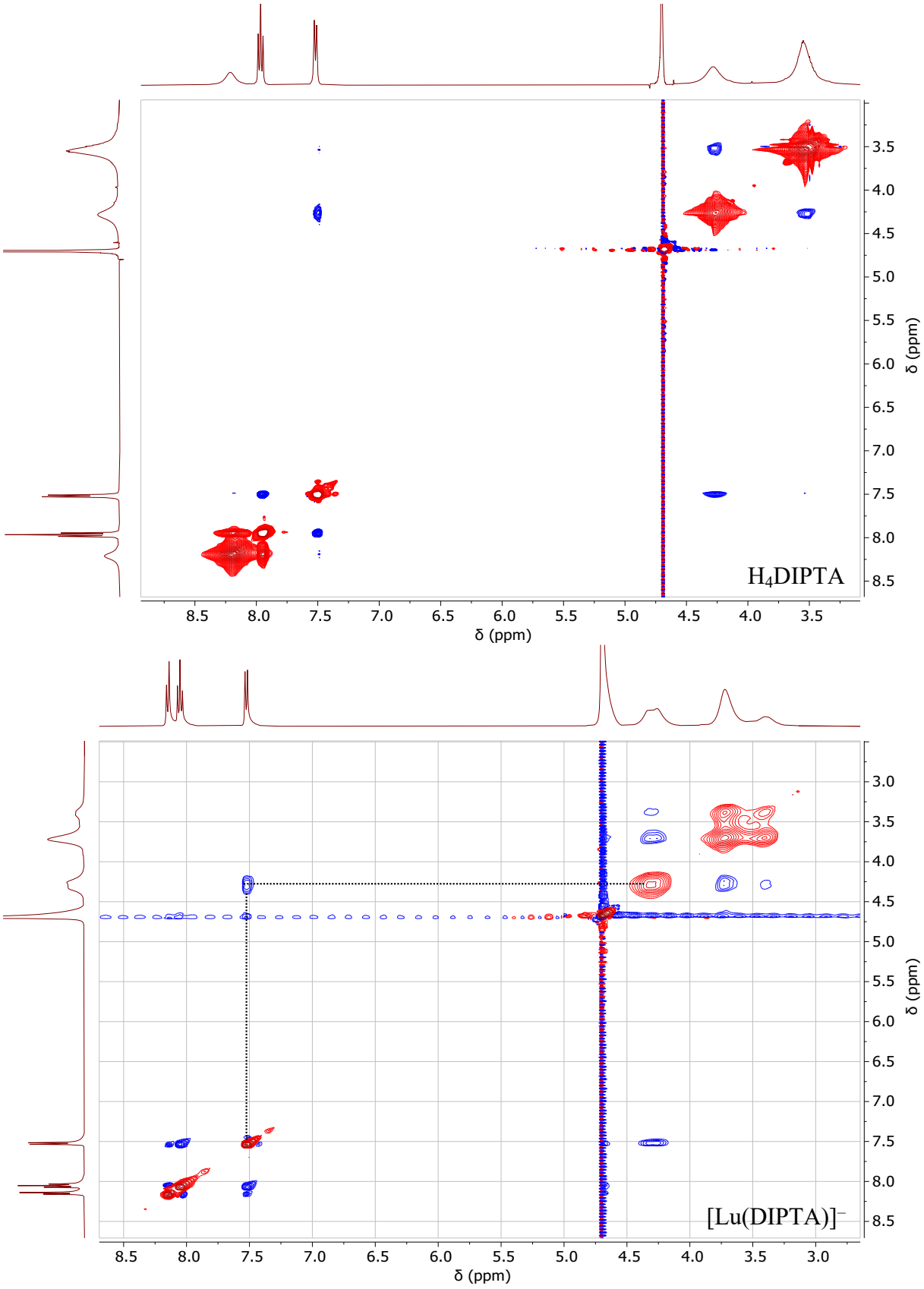

Figure S9. ^{1}H NOESY NMR spectrum of H_4DIPTA (pH=9.2, D_2O, T=298 K) and $[Lu(DIPTA)]^-$ (pH=10.0, D_2O, T=298 K)

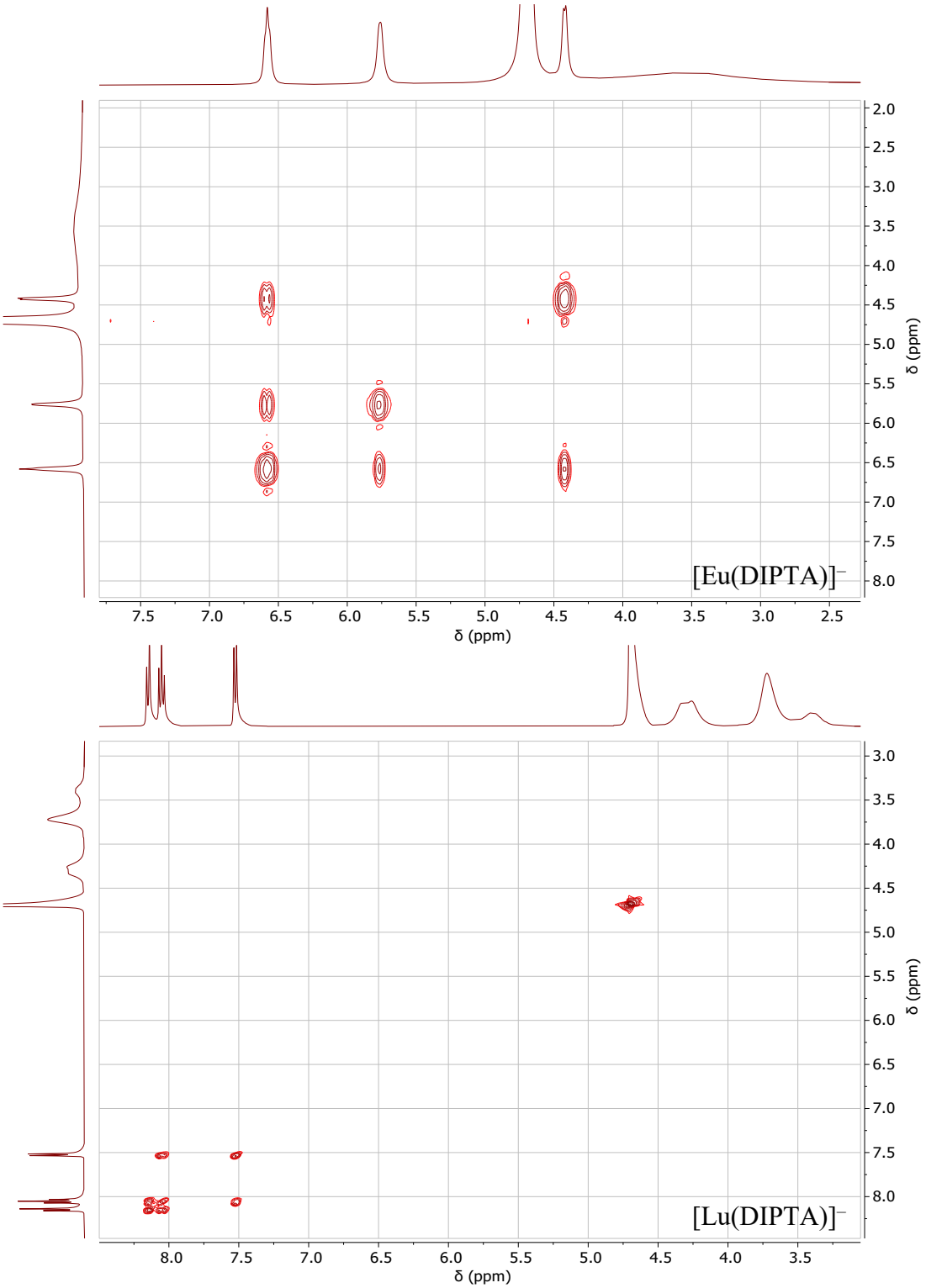

Figure S10. ^{1}H COSY NMR spectrum of [Eu(DIPTA)]$^{-}$ (pH = 6.5) and [Lu(DIPTA)]$^{-}$ (pH = 10.0) recorded at 298 K.

Assignation of the signals

The assignation of ^{1}H signals of the ligand was carried out by means of ^{1}H, ^{13}C, HMBC and NOESY measurements. In the case of the Eu(III) and Lu(III) complexes, peak integrals, NOESY and COSY spectra delivering cross peaks between protons on adjacent carbons were used for the assignment (Figure S9-S10).

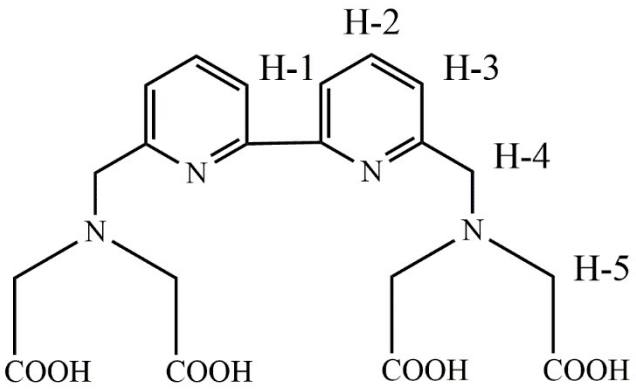

The patterns of the ^{1}H signals are very similar for the Lu[DIPTA] and the ligand, namely the ^{1}H duplet is observed at 7.5 ppm which corrsponds to one of the aromatic protons close to the aliphatic pendants (H-3). This was further confirmed by the NOESY spectrum of the complex. The aliphatic protons have been assigned according to their integrals. Furthermore, since the Eu(III) ion is paramagnetic, the relaxation processes of all protons are enhanced, thus all ^{1}H peaks are broadened.[1] The ^{1}H peak at 6.6 ppm shows the aromatic protons in the middle of the aromatic ring (H-2), while the signal of the H-3 protons is located at 4.4 ppm, since the largest paramagnetic shift must be observed for these hydrogens.

The temperature dependence of the NMR signals of the ligand (Figure S6) shows that the peaks of the aliphatic H-4 and H-5 protons as well as the H-3 aromatic one are broadened probably due to isomeric effect, which signals are narrowed at higher temperature because of the faster exchange. For the Lu(III) complex one can conclude that the signals of the aliphatic protons are mostly affected by the exchange processes and the broadening/merging of those might be the result of the presence of coordination isomers/enantiomers in solution.[2]

In the case of $[Eu(DIPTA)]^{-}$, similar phenomenon can be observed in greater extent.

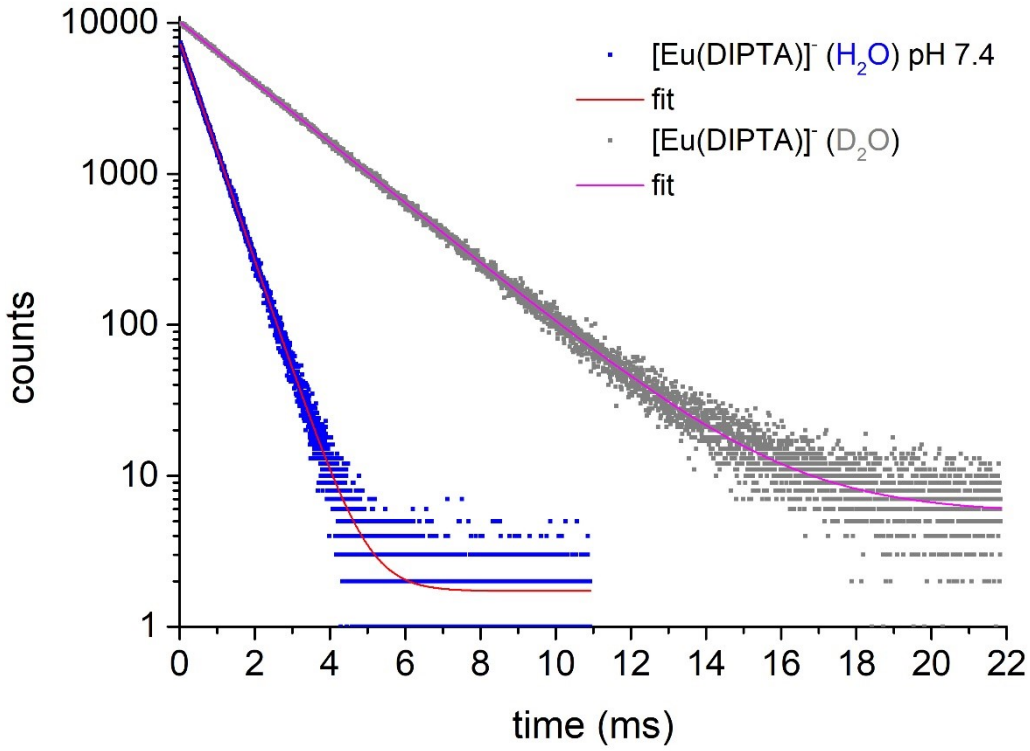

Figure S11. Decay curves recorded for $[Eu(DIPTA)]^{-}$ using time-correlated single-photon counting measurements (10^{-5} M solution, pH = 7.4, 0.1 M Tris buffer, λ_{ex} = 318 nm, λ_{em} = 613 nm).

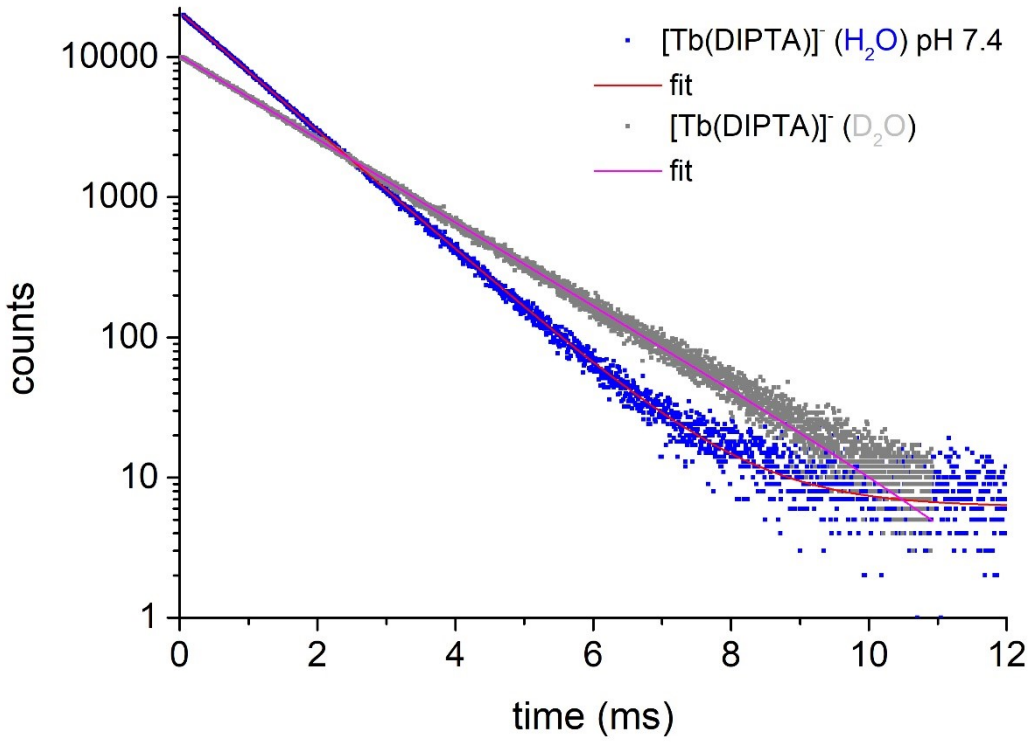

Figure S12. Decay curves recorded for $[Tb(DIPTA)]^{-}$ using time-correlated single-photon counting measurements (10^{-5} M solution, pH = 7.4, 0.1 M Tris buffer, λ_{ex} = 315 nm, λ_{em} = 542 nm).

Table S1. Energy and Cartesian coordinates of the $[Gd(DIPTA)]^-$ complex.

Electronic Energy (Eh)	-1860.18670377
Sum of electronic and zero-point Energies (Eh)	-1859.737742
Sum of electronic and thermal Energies (Eh)	-1859.701451
Sum of electronic and enthalpy Energies (Eh)	-1859.700507
Sum of electronic and thermal Free Energies (Eh)	-1859.804918
Number of Imaginary Frequencies	0

Molecular Geometry in Cartesian Coordinates

C	1.976687	1.992927	-0.920195
C	2.989440	-0.093173	-1.091473
C	4.262203	0.468933	-1.030441
C	4.372041	1.850730	-0.883640
C	3.220046	2.630817	-0.850708
C	0.680170	2.711678	-1.008472
C	-1.598870	2.442217	-1.359380
C	-1.792294	3.820702	-1.443997
C	-0.693157	4.658684	-1.271672
C	0.566648	4.102402	-1.069779
H	5.140835	-0.160596	-1.094063
H	5.346628	2.319118	-0.815177
H	3.292688	3.707837	-0.777210
H	-2.779174	4.221895	-1.639394
H	-0.811482	5.734915	-1.313475
H	1.435141	4.740056	-0.972647
N	1.879501	0.652729	-0.993419
N	-0.396351	1.910711	-1.108749
C	2.745876	-1.557282	-1.366998
H	2.356280	-1.627846	-2.386239
H	3.686552	-2.120103	-1.326626
C	-2.687797	1.435766	-1.630681
H	-3.667921	1.920999	-1.701830
H	-2.469866	0.984103	-2.602186
N	1.732061	-2.133807	-0.462489
N	-2.686675	0.359470	-0.619318
C	-3.484901	0.764274	0.549814
H	-3.301558	1.826790	0.733495
H	-4.562008	0.641268	0.378647
C	-3.161222	-0.906620	-1.213676
H	-3.261124	-1.636482	-0.404212
H	-4.137303	-0.793370	-1.701527
C	-2.134825	-1.469334	-2.220039
O	-0.911666	-1.109270	-2.020268
O	-2.535766	-2.227108	-3.107928
C	-3.065059	0.036563	1.826577
O	-2.026809	-0.697658	1.755942
O	-3.720275	0.265112	2.865207
C	1.086973	-3.316163	-1.065126
H	1.759742	-4.181882	-1.102270
H	0.792212	-3.054610	-2.084130
C	2.357764	-2.501545	0.826437
H	1.658828	-3.148031	1.364007
H	3.293688	-3.050521	0.670260
C	-0.201123	-3.689004	-0.315562
O	-0.664751	-4.822293	-0.481567
O	-0.712689	-2.756719	0.410397
C	2.605711	-1.279274	1.711618

O	1.644668	-0.408192	1.688966
O	3.628459	-1.194375	2.391473
Gd	-0.253231	-0.425820	0.158389
O	-0.427407	1.585050	1.708413
H	-0.784144	1.333868	2.598794
H	0.453141	1.981714	1.911783
O	-1.428800	0.955322	4.191784
H	-2.299454	0.594301	3.894510
H	-1.650699	1.774804	4.651759
O	2.136905	2.099986	2.443284
H	2.135787	1.121055	2.267817
H	2.759410	2.460855	1.799578

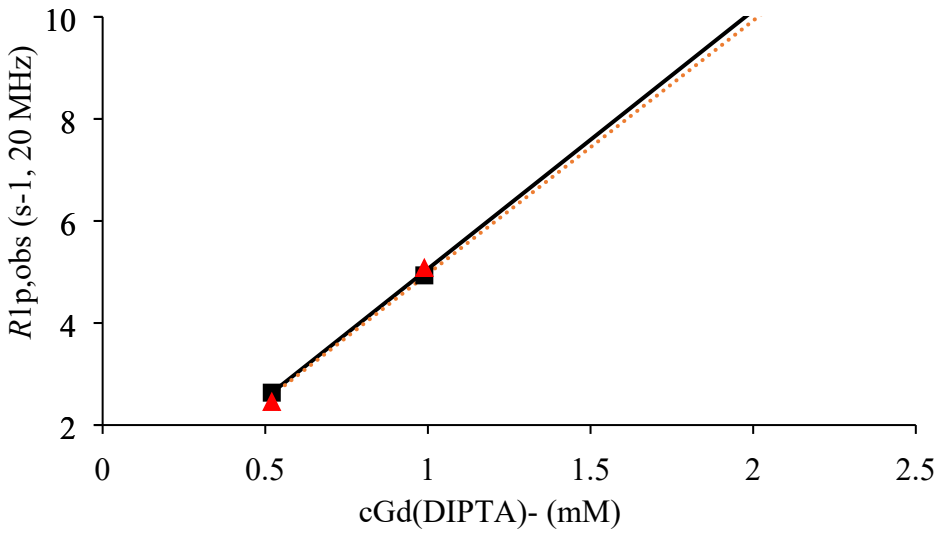

Figure S13. Determination of r_{1p} relaxivity of $[Gd(DIPTA)]^-$ at 25 °C and 37 °C (0.47 T)

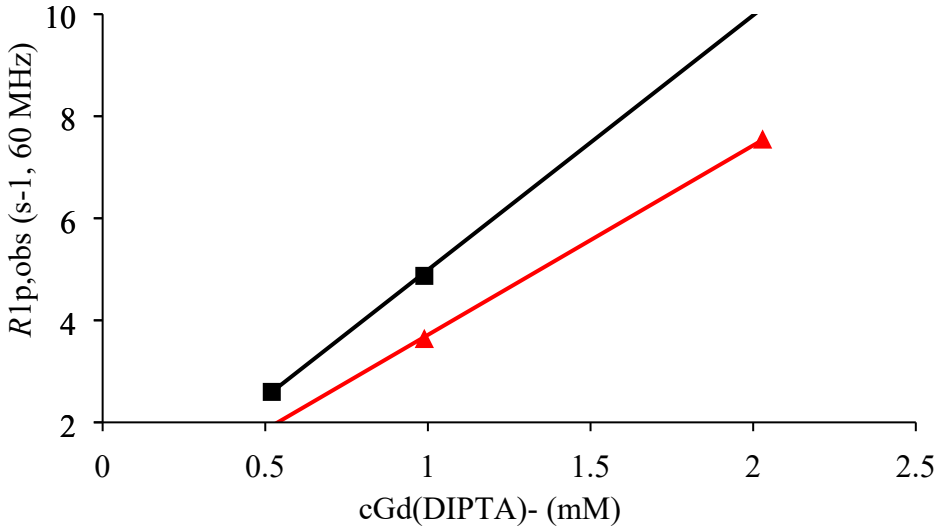

Figure S14. Determination of r_{1p} relaxivity of $[Gd(DIPTA)]^-$ at 25 °C and 37 °C (1.41 T)

Equations used for the fitting of ^{17}O NMR data

^{17}O NMR data have been fitted according to the Swift and Connick equations.[3,4] The reduced transverse ^{17}O relaxation rates, $1/T_{2r,}$ have been calculated from the measured relaxation rates $1/T_2$ of the paramagnetic solutions and from the relaxation rates $1/T_{2A}$ of the diamagnetic reference:

$$\frac{1}{T_{2r}} = \frac{1}{P_m}\left[\frac{1}{T_2} - \frac{1}{T_{2A}}\right] = \frac{1}{\tau_m}\frac{T_{2m}^{-2} + \tau_m^{-1}T_{2m}^{-1} + \Delta\omega_m^2}{(\tau_m^{-1} + T_{2m}^{-1})^2 + \Delta\omega_m^2} \qquad \text{(S1)}$$

$\Delta\omega_m$ is determined by the hyperfine or scalar coupling constant, $A_O/\square$, where B represents the magnetic field, S is the electron spin and g_L is the isotropic Landé g factor (Equation (S2)).

$$\Delta\omega_m = \frac{g_L\mu_B S(S+1)B}{3k_B T}\frac{A_O}{\mathsf{h}} \qquad \text{(S2)}$$

The ^{17}O transverse relaxation rate is mainly determined by the scalar contribution, $1/T_{2sc}$, and it is given by Equation (S3).

$$\frac{1}{T_{2m}} \cong \frac{1}{T_{2sc}} = \frac{S(S+1)}{3}\left(\frac{A_O}{\mathsf{h}}\right)^2 \tau_s \qquad \frac{1}{\tau_s} = \frac{1}{\tau_m} + \frac{1}{T_1} \qquad \text{(S3)}$$

The exchange rate, k_{ex}, (or inverse binding time, τ_m) of the inner sphere water molecule is assumed to obey the Eyring equation (Equation (S4)) where $\Delta S^{\ddagger}$ and $\Delta H^{\ddagger}$ are the entropy and enthalpy of activation for the exchange, and $^{298}k_{ex}$ is the exchange rate at 298.15 K.

$$\frac{1}{\tau_m} = k_{ex} = \frac{k_B T}{h}\exp\left\{\frac{\Delta S^{\ddagger}}{R} - \frac{\Delta H^{\ddagger}}{RT}\right\} = \frac{k_{ex}^{298}T}{298.15}\exp\left\{\frac{\Delta H^{\ddagger}}{R}\left(\frac{1}{298.15} - \frac{1}{T}\right)\right\} \qquad \text{(S4)}$$

For the fit of the ^{17}O T_2 data, we used an exponential function to treat the temperature dependency of $1/T_{1e}$:

$$\frac{1}{T_{1e}} = \frac{1}{T_{1e}^{298}} \exp\left\{\frac{E_v}{R}\left(\frac{1}{T} - \frac{1}{298.15}\right)\right\} \quad \text{(S5)}$$

References

(1) *The Chemistry of Contrast Agents in Medical Magnetic Resonance Iaging*, Second edition.; Merbach, A. E., Helm, L., Tóth, É., Eds.; Wiley: Chichester, West Sussex, 2013.

(2) Aime, S.; Botta, M.; Ermondi, G. NMR Study of Solution Structures and Dynamics of Lanthanide(III) Complexes of DOTA. *Inorg. Chem.* **1992**, *31* (21), 4291–4299. https://doi.org/10.1021/ic00047a016.

(3) Swift, T. J.; Connick, R. E. Erratum: NMR-Relaxation Mechanisms of ^{17} O in Aqueous Solutions of Paramagnetic Cations and the Lifetime of Water Molecules in the First Coordination Sphere. *J. Chem. Phys.* **1964**, *41* (8), 2553–2554. https://doi.org/10.1063/1.1726303.

(4) Swift, T. J.; Connick, R. E. NMR-Relaxation Mechanisms of O ^{17} in Aqueous Solutions of Paramagnetic Cations and the Lifetime of Water Molecules in the First Coordination Sphere. *J. Chem. Phys.* **1962**, *37* (2), 307–320. https://doi.org/10.1063/1.1701321.